Electronic Supplementary Material (ESI) for Journal of Materials Chemistry A.

Promoting polysulfide conversion by catalytic separator with $LiNiPO_4$ and rGO hybrids for high performance lithium–sulfur batteries

Yinze Zuo[a,b], Yuejin Zhu[a,d], Qi Wang[a,b], Kezhong Lv[a,b], Weiming Su[a,b], Yuefeng Tang[a,b,c] and Yanfeng Chen[a,b]*

[a]National Laboratory of Solid State Microstructures, Jiangsu Key Laboratory of Artificial Functional Materials, College of Engineering and Applied Sciences, Nanjing University, Nanjing, China.
[b]Collaborative Innovation Center of Advanced Microstructures, Nanjing University, Nanjing, China.
[c]SuZhou Sun Sources Nano Science and Technology Co. Ltd., ChangShu, SuZhou 215513, China.

[d]Institute of Advanced Synthesis, School of Chemistry and Molecular Engineering, Nanjing Tech University, Nanjing, China.
*E-mail: yftang@nju.edu.cn

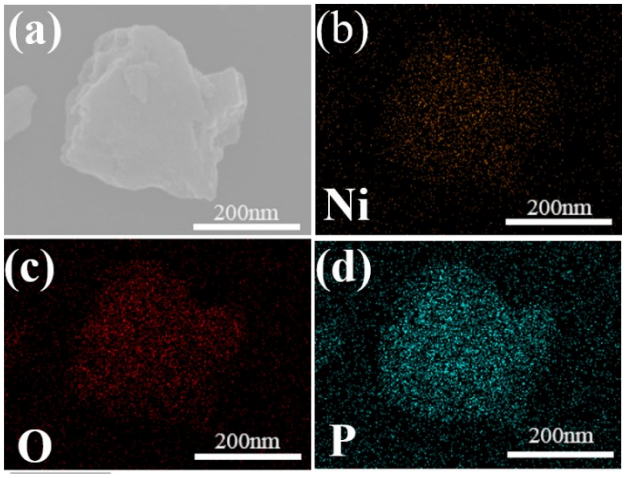

Fig. S1. The SEM image of LNPO and corresponding EDS mapping of Ni, O and P.

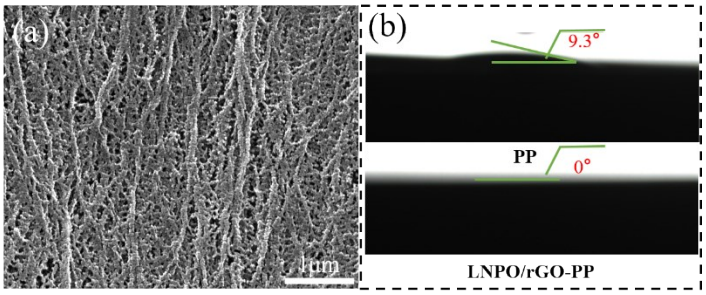

Fig. S2. (a) The SEM image of pristine separator and (b) surface wetting of electrolyte droplets on the pristine separator (PP) and LNPO/rGO modified separator.

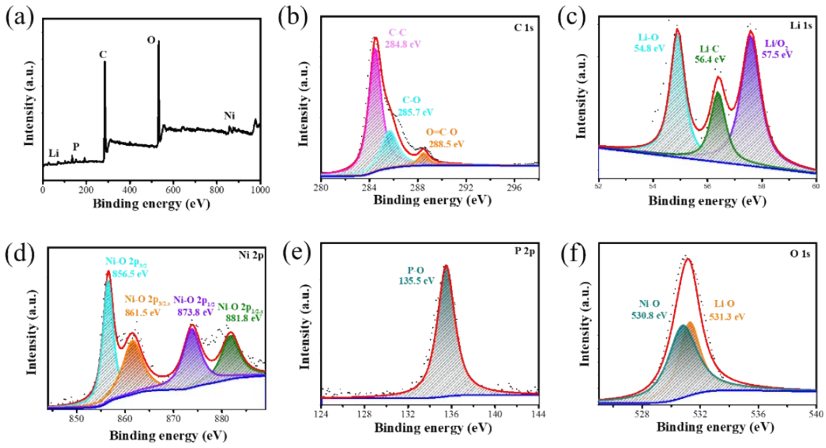

Fig. S3. (a)XPS and HRXPS spectra of the C 1s, Li 1s, Ni 2p, P 2p, O 1s in LNPO/rGO hybrids.

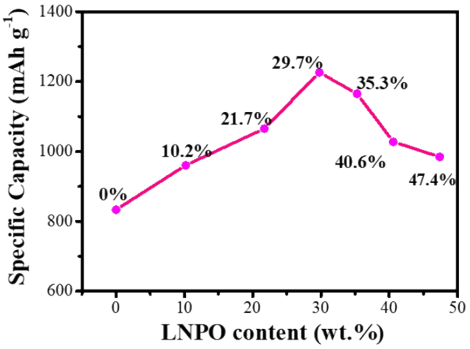

Fig. S4. Capacity optimization of LNPO content in the LNPO/rGO modified separator.

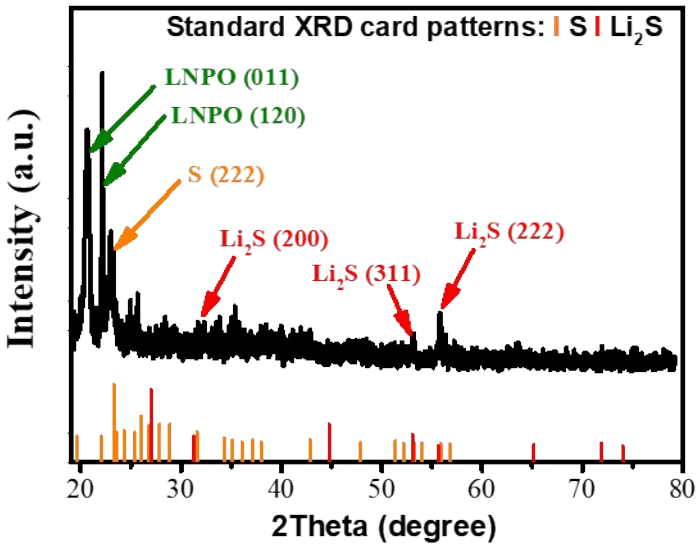

Fig. S5. XRD pattern of LNPO/rGO modified separator after cycling and standard XRD patterns sulfur and Li_2S powder.

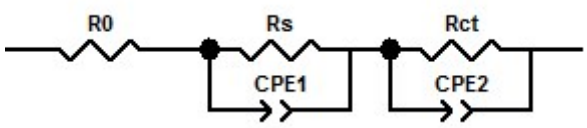

Fig. S6. The equivalent circuit diagram of the Nyquist plots.

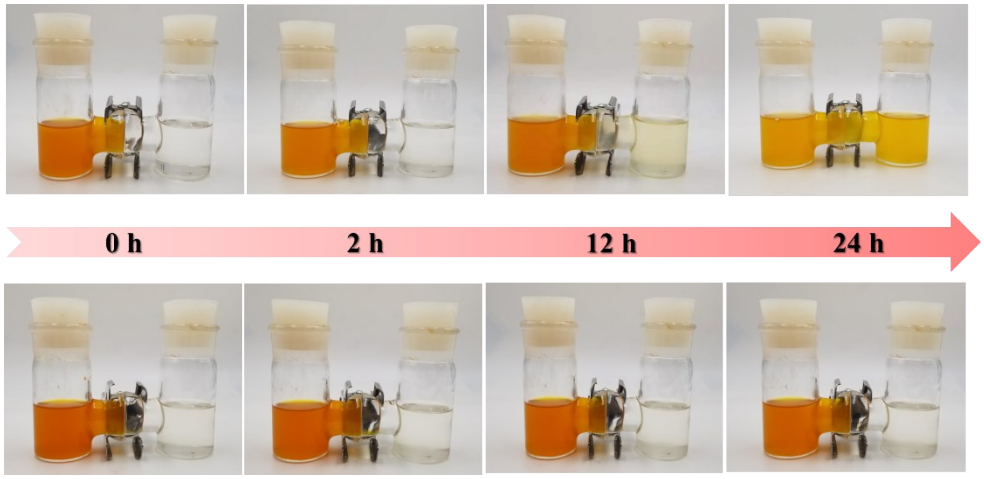

Fig. S7. Digital photographs of the Li_2S_6 diffusion tests for the pristine separator (top) and LNPO/rGO modified separator (bottom)

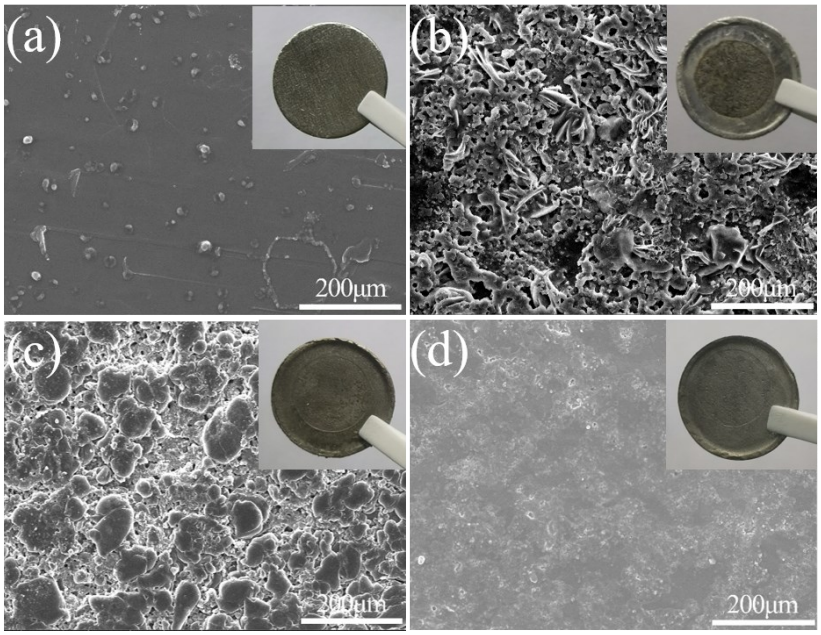

Fig. S8. (a) SEM images of the surface of (a) the pristine Li metal; the surface of Li metals in the cell with the (b) pristine separator, (c) rGO modified separator and (d) LNPO/rGO modified separator after cycling.

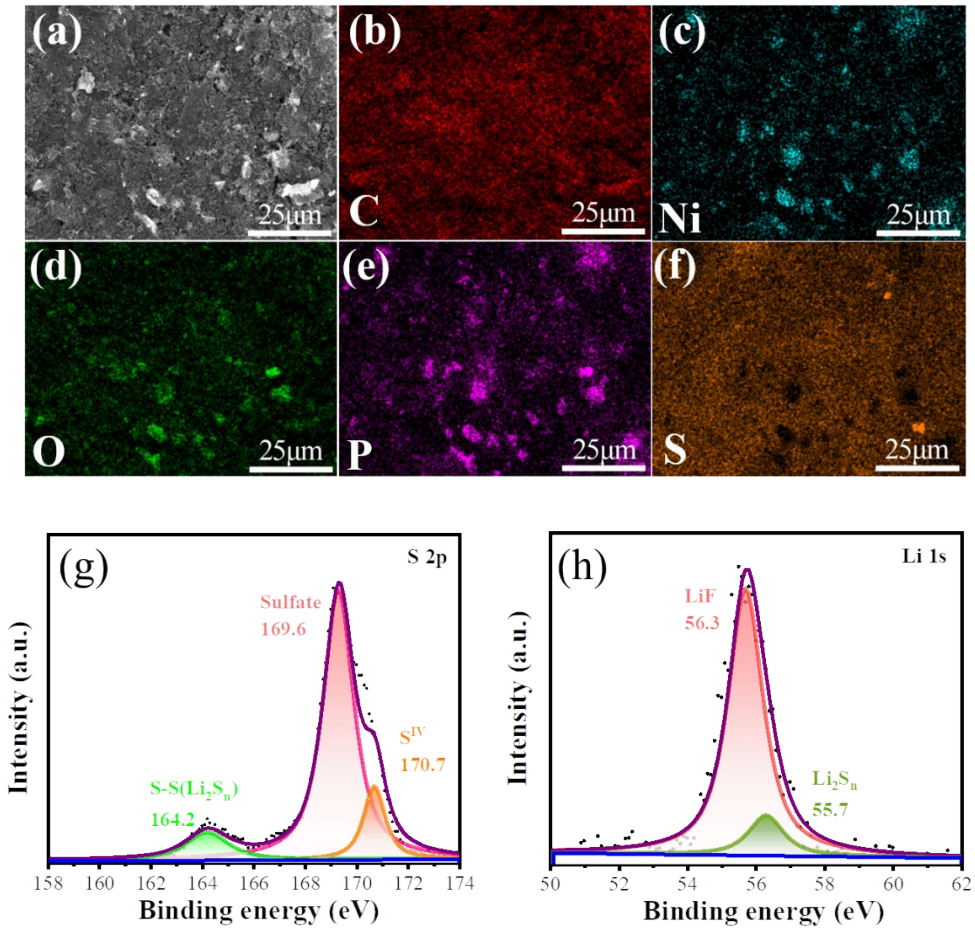

Fig. S9. (a) SEM image and corresponding elemental mapping images of (b) C, (c) Ni, (d) O, (e) P and (f) S elements of the LNPO/rGO modified separator after cycling and HRXPS spectra of (g) S 2p; and (h) Li 1s of the LNPO/rGO modified separator after cycling.

Table S1. Comparison of electrochemical properties functional separators in Li–S cells

Coating or interlayer	Sulfur loading (mg cm^{-2})	Sulfur content (%)	Cycle number	Reversible capacity (mAh cm^{-2})	Capacity retention (%)	Ref
MoO_3/CNT	1	60	400	655	55	S1
Cu_2(CuTCPP)	2	70	900	604	71	S2
MoO_2/Mo_2N	1.1	70	900	461	58	S3
GA/CNFs/Ni	1.5	90	500	620	71	S4
CNFs/VS_4	1.25	80	600	520	57	S5
AC/Ni/N	2	80	700	575	65	S6
LNPO/rGO	1.5	80	1400	629	67	This work

Table S2. Comparison of electrochemical properties functional separators in Li–S cells with high sulfur loading

Coating or interlayer	Sulfur loading (mg cm^{-2})	Sulfur content (%)	Cathode	Discharge Capacity (mAh g^{-1})	Areal capacity (mAh cm^{-2})	Electrolyte/ Sulfur ratio	Ref
GO@MoS_2	3.64	70%	CB/S	~600 mAh g^{-1}, 95th, 0.2 C	2.2	14	S7
SSNS/CNT	1.0	65%	KB/S	680 mAh g^{-1}, 100th, 0.2 C	<2.0	N/A	S8
CNF@ZrO_2	2.7	70%	CB/S	800 mAh g^{-1}, 60th, 0.2 C	~2.1	40	S9
TiN	1.3	70%	Super P/S	744 mAh g^{-1} 200th, 0.5 C	<2.0	46	S10
g-C_3N_4	4.0	45%	GO/S	~600 mAh g^{-1}, 60th, 0.2 C	~2.4	20	S11
CoP	3.24	56%	rGO/S	~800 mAh g^{-1}, 100th, 0.2 C	~2.7	N/A	S12
LNPO/rGO	6	80%	CB/S	~623 mAh g^{-1}, 300th, 0.3 C	4.2	8.3	This work

Table S3. The impedance parameters simulated from the equivalent circuit fitting of different cells

Sample	R_o(Ω)	R_{ct}(Ω)
LNPO/rGO	23.17	517
rGO	56.32	1853

[S1] L. Y. Luo, X. Y. Qin, J. X. Wu, G. M. Liang, Q. Li, M. Liu, F. Y. Kang, G. H. Chen, B. H. Li, An interwoven MoO_3@CNT scaffold interlayer for high-performance lithium-sulfur batteries, *J. Mater. Chem. A*, **2018**, 6, 8612-8619.

[S2] M. Tian, F. Pei, M. S. Yao, Z. H. Fu, L. L. Lin, G. D. Wu, G. Xu, H. Kitagawa, X. L. Fang, Ultrathin MOF nanosheet assembled highly oriented microporous membrane as an interlayer for lithium-sulfur batteries, *Energy Storage Mater.* **2019**, 21, 14-21.

[S3] J. L. Yang, S. X. Zhao, Y. M. Lu, X. T. Zeng, W. Lv, G. Z. Cao, In-situ

topochemical nitridation derivative MoO_2–Mo_2N binary nanobelts as multifunctional interlayer for fast-kinetic Li-Sulfur batteries, *Nano energy*, **2020**, 68, 104356.

[S4] Y. Zhang, R. Wang, W. Tang, L. Zhan, S. Zhao, Q. Kang, Y. Wang, S. Yang, Efficient polysulfide barrier of a graphene aerogel-carbon nanofibers-Ni network for highenergy-density lithium-sulfur batteries with ultrahigh sulfur content, *J. Mater. Chem. A*, **2018**, 6, 20926-20938.

[S5] Y. Zhang, G. Xu, Q. Kang, L. Zhan, W. Tang, Y. Yu, K. Shen, H. Wang, X. Chu, J. Wang, S. Zhao, Y. Wang, L. Ling, S. Yang, Synergistic electrocatalysis of polysulfides by a nanostructured VS_4-carbon nanofiber functional separator for high-performance lithium-sulfur batteries, *J. Mater. Chem. A*, **2019**, 7, 16812-16820.

[S6] Y. Zuo, M. Zhao, P. Ren, W. Su, J. Zhou, Y. Chen, Y. Tang, Y. Chen, An efficient polysulfide trapper of an nitrogen and nickel-decorating amylum scaffold-coated separator for ultrahigh performance in lithium-sulfur batteries, *J. Mater. Chem. A,* **2020**, 8, 1238-1246.

[S7] L. Tan, X. H. Li, Z. X. Wang, H. J. Guo, J. X. Wang, Lightweight reduced graphene oxide@MoS_2 interlayer as polysulfide barrier for high-performance lithium-sulfur batteries, *ACS Appl. Mater. Interfaces*, **2018**, 10, 3707-3713

[S8] S. S. Yao, J. C, J. Q. Huang, Z. H. Lu, Y. Deng, W. G. Chong, J. X. Wu, M. Haq, F. Ciucci, J. K. Kim, Novel 2D Sb_2S_3 nanosheet/CNT coupling layer for exceptional polysulfide recycling performance, *Adv. Energy Mater.,* **2018**, 1800710.

[S9] Y. Li, J. Zhu, R. Shi, M. Dirican, P. Zhu, C. Yan, H. Jia, J. Zang, J. He, X. Zhang, Ultrafine and polar ZrO_2-inlaid porous nitrogen-doped carbon nanofiber as efficient polysulfide absorbent for high-performance lithium-sulfur batteries with long lifespan, *Chem. Eng. J.,* **2018**, 349, 376-387.

[S10] B. Y. Hao, H. Li, W. Lv, Y. B. Zhang, S. Z. Niu, Q. Qi, S. J. Xiao, J. Li, F. Y. Kang, Q. H. Yang, Reviving catalytic activity of nitrides by the doping of the inert surface layer to promote polysulfide conversion in lithium-sulfur batteries, *Nano Energy*, **2019**, 60, 305-311.

[S11] Y. Huang, T. Zheng, K. Zhang, X. She, H. Xu, Z. Fang, K. Xie, Facile fabrication of permselective g-C_3N_4 separator for improved lithium-sulfur batteries, *Electrochim.*

Acta, **2018**, 272, 60-67.

[S12] X. X. Chen, X. Y. Ding, C. S. Wang, Z. Y. Feng, L. Q. Xu, X. Gao, Y. J. Zhai, D. B. Wang, A multi-shelled CoP nanosphere modified separator for highly efficient Li–S batteries, *Nanoscale*, **2018**, 10, 13694.